ADVANCED MATERIALS
www.advmat.de

Room Temperature Homogeneous Ductility of Micrometer-sized Metallic Glass

Dominik Tönnies, Robert Maaß, and Cynthia A. Volkert**

An elastic–plastic response of an engineering material is the key for safe structural design, and forms the success of crystalline metals we meet in daily use. The discovery of glassy metals with a disordered atomic structure was the advent of a new class of advanced materials with outperforming physical properties but the caveat that they lack tensile ductility. In fact, metallic glasses (MG) are known to deform via shear localization and structural softening, resulting in quasi-brittle failure that undercuts their potential for engineering solutions. However, at the nano-scale a different, more ductile deformation mode is observed, opening avenues to exploit a high-strength elastic–plastic material for structural applications in the field of miniaturized devices. This change in deformation mode, reminiscent of MGs high temperature deformation, is a puzzling and poorly understood phenomenon of a material that is micro structurally defined at the atomistic scale. In this communication, we present clear evidence for how the spacing of mesoscopic shear defects determines the size-induced brittle-to-ductile transition at small scales. We furthermore demonstrate that the transition in flow mode is rate dependent without a change in the underlying atomistic deformation mechanism. Our results extend the envelope of strong-but-ductile behavior under quasi-static deformation to the micrometer regime and therefore also to a length scale relevant for micro-electromechanical (MEMS) applications.

Tremendous research efforts have highlighted the outstanding performances of MGs. Properties that classify them among the most promising engineering materials are a high elastic limit in combination with high strength,[1] strong wear and corrosive resistance,[2] as well as superior soft-magnetic behavior.[3] Given these advantages, why don't we see them in daily applications? Two main caveats are still hampering mass application. Those are suitable near-net shape production routes, as well as their lack of ductility — a property structural applications are crucially reliant on. Whilst recent breakthroughs in processing are offering new pathways for mass production,[4,5] the intrinsic propensity for catastrophic failure is a remaining challenge. With some exceptions, monolithic MGs at low homologous temperatures ($T/T_g < 0.8$, with T_g being the glass transition temperature) are brittle in tension but may show compressive ductility.[1] In both deformation modes, plastic strain and failure is mediated by the formation of nanoscopic planar defects, called shear bands. This shear localization is difficult to assess experimentally due to its confinement to some tens of nanometers,[6] and due to the short (~ms at ambient conditions) operating time scales.[7,8] Many efforts have thus been dedicated to understanding shear-band dynamics,[9–11] shear-band structure,[12,13] as well as increasing the shear-band density and therefore plastic strain prior to failure. The latter can for example be done by MG-composite design,[14] tuning of Poisson's ratio,[15] but can also be a result of non-uniaxial stress states during deformation.[16,17] More recently, the emergence of micro- and nano-mechanical testing abilities demonstrated yet another route to improve ductility of monolithic MGs: the simple reduction of extrinsic length-scales clearly yields not only increased ductility but also an apparent transition in deformation mode from shear-localization to homogeneous-like flow.[18–22] In stress-strain data the transition manifests itself as a change from intermittent flow via shear-banding to a smooth and apparent homogeneous deformation mode.

Qualitatively first shown by Guo et al. inside a transmission electron microscope (TEM), a Zr-based metallic glass can exhibit tensile ductility when extrinsic dimensions are reduced to some hundred nm.[23] More quantitatively, Volkert et al. reported a distinct change from shear-band dominated plastic flow of amorphous $Pd_{77}Si_{23}$ micro- and nano-columns to homogeneous deformation when the specimen diameter decreased below a certain value around ~400 nm.[18] This unexpected transition in flow response was successfully motivated by comparing the energy balance between the change in elastic strain energy and shear-band energy. Subsequently, various reports on similar measurements, but different metallic glasses reported intriguingly contradicting results: both micro-compression on Pd-based and Zr-based MG showed no change in deformation made across sample sizes between 250 nm and several micrometers, with shear-banding as the dominant deformation mechanism.[24,25] In-situ TEM experiments convey a similar picture for a Zr- and a Cu-based MG in compression down to an experimentally accessible size of about 100 nm, but more interestingly, they allow observation of homogeneous deformation upon bending of a 200 nm large specimen.[20] In yet another work by Jang et al., a change in deformation mode from localized-intermittent to homogeneous behavior is found for a Zr-based MG.[19] The results in Ref.[19] and [20] are based on electron imaging, where shear-offsets typical for shear-banding are absent within the resolution of the method. This is of particular interest, since the flow curve in figure 5c of Ref.[19] clearly suggests a repeated shear-band activation, as is known for the stick-slip like flow dynamics of MG.[26] A very large apparent size (ca. 300 nm) at which the deformation mode changes from intermittent shear-banding to apparent

D. Tönnies, Dr. R. Maaß, Prof. C. A. Volkert
University of Göttingen
Institute of Materials Physics
Friedrich-Hund-Platz 1, 37077 Göttingen, Germany
E-mail: robert.maass@ingenieur.de;
volkert@ump.gwdg.de

DOI: 10.1002/adma.201401123

homogeneous flow has been found for an Al-based MG.[21] In this case, flow commences via shear-banding, as is again visible in the associated load-displacement curves (Ref. [21], Figure 3), but continues further in a smooth fashion.

Why are all these reports of such variation? Which factors influence the apparent flow response, and is there an intrinsic change in the flow behavior?

Whilst many questions related to this size-effect are yet to be unraveled, a recent report by Magagnosc et al. shed some light on the change in flow behavior at small length scales.[27] As is known since the 80s for bulk MG specimen, irradiation can be used to repeatedly alternate between a brittle and ductile state.[28,29] Similarly, Magagnosc et al. could demonstrate the change from "brittle-to-ductile" tensile behavior upon ion-irradiation. More specifically, these authors use as-cast glassy nano-wires, which are exposed to Ga^+-ions from focused ion beam (FIB) in order to change from "brittle" to quasi-homogeneous flow. Given that the above contradicting reports in search of the size-dependent cross-over in flow behavior all employ FIB for sample preparation, it seems clear that the preparation method may be one of the factors responsible for the apparent "brittle-to-ductile" transition. Further support for this irradiation induced "brittle-to-ductile" transition in small scale systems is given by molecular dynamics (MD) simulations,[30]

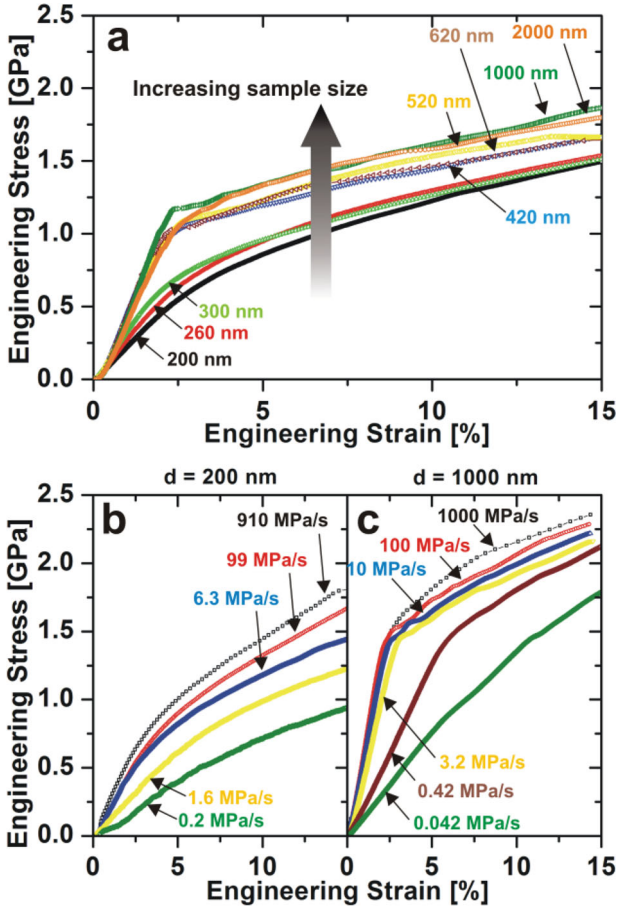

Figure 1. a) Engineering stress-strain data as a function of sample size. b) and c) Engineering stress-strain data as a function of stress rate for columns with diameters of (b) 200 nm and (c) 1000 nm.

where the suppression of shear-banding is explained by irradiation induced atomic scale (re)disordering that is characterized by the average potential energy of the system.

With this at hand, one may argue that the final answer to the size-affected apparent "brittle-to-ductile" transition is indeed an artifact from the FIB preparation method, where different outcomes are due to the underlying resistance against Ga^+-irradiation of various chemically and structurally different MGs.

In this work, we propose a mechanism that has a quite different origin, and that also can be observed at much larger sample sizes, where the volume fraction of irradiated surface material is irrelevant: the long known decrease in shear-band spacing with sample size across numerous length scales[31] converges towards a value that effectively leads to a homogenization effect at the length scales concerned. As will be shown in the following, we argue that the apparent "brittle-to-ductile" (in the following termed "intermittent-to-homogeneous") transition in small scale MG-specimen can be understood as a result of the shear-band spacing approaching the shear-band thickness. We further support this finding with rate dependent measurements that exhibit monotonous positive strain rate sensitivity across all length scales, underlining that there is no overall change in deformation mechanism. Finally, we summarize the dominance of intermittent shear-banding or smooth flow in a rate-size deformation map revealing that apparent homogeneous flow behavior can be observed at sample sizes as large as 1 µm.

The representative size-dependent stress-strain behavior measured at comparable rates (10–100 MPa/s) for columns of diameters between 200 nm and 2000 nm is displayed in **Figure 1**a. At least 9 samples per nominal size bin (200, 250, 300, 400, 500, 600, 1000 and 2000 nm) were tested. For sample sizes larger than about 420 nm, a clear transition between the elastic and plastic flow regime at a size-independent stress of about 1.1–1.2 GPa is observed. In this size-regime, displacement jumps during plastic deformation are also seen (Figure 1a), which is known to correspond to the intermittent kinetics of shear-banding during serrated flow.[10,26] Samples smaller than 300 nm in diameter exhibit a distinctly different stress-strain response: strain-jumps are absent within the first ~15% of strain and the transition to plastic flow sets in at much lower stresses. Thus, as gleaned from the flow behavior, Figure 1a is very much in agreement with previous reports on an intermittent-to-homogeneous transition.[18–22]

Whilst Figure 1a reproduces known deformation physics of small-scale MG specimen, Figure 1b and 1c illustrate an unexpected stress-rate sensitivity for both the lower (200 nm, 41 tests) and upper end (1000 nm, 36 tests) of the studied size range. The data in Figure 1b and 1c highlight exemplarily the rate sensitivity for loading rates covering a range of four to five orders of magnitude. It is noted that the stress rate can be directly translated into a strain rate, and that this observed (strain)-rate sensitivity is different from the room temperature behavior of bulk MGs. Rate dependencies at the micro- and nano-scale have, to the authors best knowledge, not been addressed so far, but are well characterized at the macroscopic scale, where MGs generally show a negligible or apparent negative strain-rate sensitivity due to dynamic velocity weakening during inhomogeneous flow.[32] This is not the case in the data of our nano- and

Adv. Mater. **2014**,
DOI: 10.1002/adma.201401123

micro-scaled specimens presented in Figure 1b and 1c. In fact, with decreasing applied rate, the samples tend to become softer. It is evident that the decreasing rate enhances the apparent soft and smooth flow response of the 200 nm specimen already seen in Figure 1a. Even the 1000 nm columns show a considerable rate-dependent stress-strain response: the clearly distinguishable separation between the elastic and plastic part of the response vanishes with decreasing applied rate (Figure 1c). This is particularly interesting, since the low slope of the first part of the stress-strain curve for very small samples is often associated with the inevitable top-rounding that originates from the FIB-milling procedure.[24] As a result, small samples (<300 nm) in such tests are said to deform plastically at a lower engineering stress, because the true stress is much higher at the small contact surface between the rounded top and the compression anvil. The absolute value of the top-rounding curvature radius due to the FIB-processing is fairly constant or decreases slightly with increasing sample size and can be considered to be negligible at a column diameter of 1000 nm, which also yields a distinct elastic–plastic behavior with measured moduli approaching the known material values. Thus, Figure 1c demonstrates that the low apparent elastic slope can equally well be a result of a low applied rate. We note that a change of elastic slope as a function of sample size is unexpected, and certainly not due to size-dependent elasticity. Nevertheless, the reproducibility of the stress-strain data as depicted in Figure 1 suggests a trend unaffected by the boundary conditions of the test, and is attributed to the emergence of the apparent homogenous deformation mode. Since it is known that extraction of elastic properties from small scale experiments is suffering from numerous artifacts,[24,33] we explicitly avoid any determination of such parameters. We discuss further details of the relevant boundary conditions of the experiments in the Supporting Information (SI).

The rate effect seen in Figure 1b and 1c can be further supported by investigating the deformed specimens with scanning electron microscopy (SEM), of which a rate dependent image series for 1000 nm sized columns are shown in **Figure 2**a–f, and for 200 nm sized columns in Figure 2g–k. For both sample sizes a transition to an apparently homogeneous deformation behavior can be observed at stress rates of ~1 MPa/s and lower. It has to be noted that the images displayed in Figure 2 are representative of the samples after deformation to about 30% plastic strain, whereas the stress-strain data in Figure 1 focuses on the first 15% plastic strain with an emphasis on the elastic–plastic transition.

At this stage, our data thus demonstrates (i) a transition in the apparent deformation behavior with decreasing specimen size, as well as (ii) a rate-dependent softening, which is at odds with bulk MG behavior in the inhomogeneous deformation regime. In fact, such a rate dependence is only known for homogeneous deformation at high temperatures.[34] To further quantify this unexpected rate dependence we calculate the strain-rate sensitivity (SRS) m for all compression tests of columns with sizes of 200 nm and 1000 nm. The SRS exponent m is evaluated via:

$$m = \left.\frac{\mathrm{d}\log(\sigma_f)}{\mathrm{d}\log(\dot{\varepsilon})}\right|_{\varepsilon_{pl}=5\%} \quad (1)$$

at a plastic strain of $\varepsilon_{pl} = 5\%$ with σ_f being the flow stress that is derived at the column top, where plastic flow initiates, and $\dot{\varepsilon}$ is the strain rate. The actual strain rate at 5% plastic strain is evaluated by linearizing the displacement data at that strain. Further, the elastic contribution of the strain has been subtracted under the assumption that the elastic modulus amounts to 86 GPa, which was determined with Berkovich nanoindentation. **Figure 3**a displays the resulting flow strength at 5% plastic strain as a function of applied strain rate. A linear fit yields a SRS exponent $m = 0.05$ for columns of both sizes over the entire range of loading rates and *irrespective* of apparent deformation

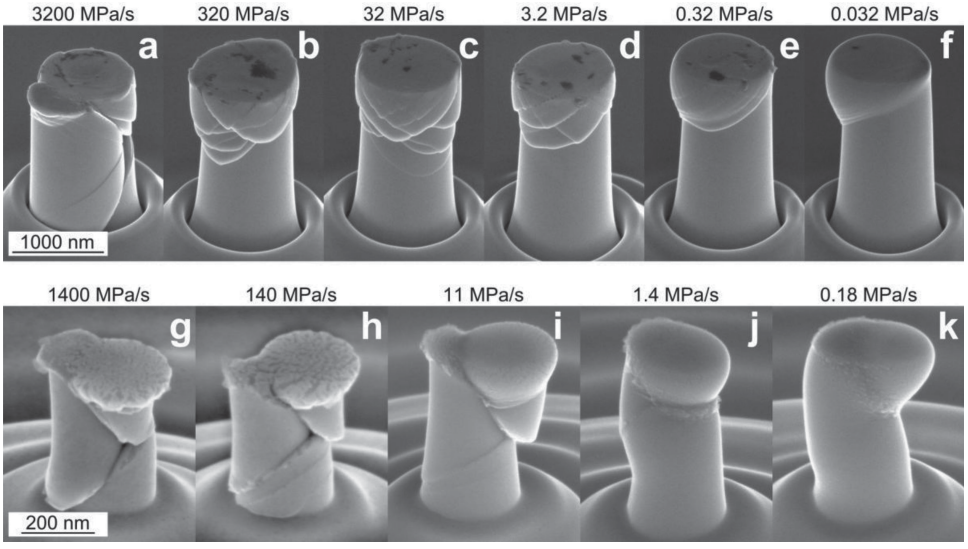

Figure 2. a–f) Morphology of deformed columns (d = 1000 nm) with decreasing stress rates from left to right. Deformation appears predominantly homogeneous at stress rates of 0.32 MPa/s and lower. g–k) Morphology of deformed columns (d = 200 nm) with decreasing stress rates from left to right. Deformation appears predominantly homogeneous at stress rates of 11 MPa/s and lower.

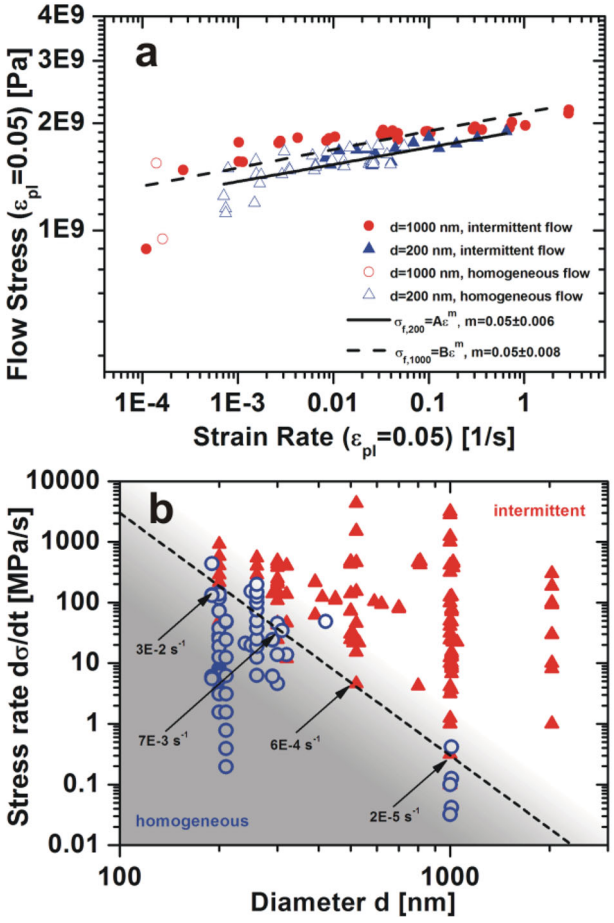

Figure 3. a) Flow stress as a function of the strain rate at a plastic strain of 5%. A strain rate exponent of m = 0.05 can be evaluated regardless of applied rates, specimen sizes and apparent deformation mode; b) regimes of intermittent and apparent homogeneous in a rate-size deformation map including more than 300 specimen investigated. The empirical boundary between the two regimes can be described by a power-law. Plastic strain rates at the transition are indicated for four different sample sizes.

mode. The range of accessible loading rates is limited by the thermal stability of the testing device at the lower end (experimental displacement rates approaching drift rate values), and by the data acquisition rate at the upper end (500 Hz). We note that despite an increase in scatter in the low strain rate regime, there is no indication of a change in SRS within a constant size series as well as among different sample sizes. Thus, at this constant testing temperature there is an apparent difference in the flow response, but no indication for a change in the underlying atomistic deformation mechanism, which one would expect to yield a change in m.[35]

Mapping the occurrence of intermittent and apparent homogeneous flow in a rate-size deformation map provides an empirical boundary between the two flow modes (Figure 3b) that may be described with a power-law of type $\dot{\sigma} \propto A \times d^{-k}$, where A is a numerical pre-factor, d the sample diameter and $k \approx 4$. The rate-dependent intermittent-to-homogeneous transition is thus highly sensitive to the applied rate, which makes the homogeneous regime inaccessible with conventional techniques at higher diameters. At the transition between localized and homogeneous flow the plastic strain rate, $\dot{\varepsilon}_{pl}$, was evaluated at 5% strain, and yields a power-law with a very similar exponent as the stress-rate boundary. The nominal plastic strain rates are indicated along the power-law line in Figure 3b.

In addition to the strain-rate dependence, the shear-band morphology of all samples tested within the same rate range (10–100 MPa/s) has been studied. This is motivated by the self-similar shear-band patterns across the size range 500–2000 nm. The number of shear-bands was thus determined from SEM images for the 500 nm samples and larger. Smaller samples were not included, because of increasing uncertainties in discriminating shear-band lines close to the apparent intermittent-to-homogeneous transition. Using the reported angular value α of about 50 ± 4° between the loading axis and the shear-band normal,[18] an estimation of the shear-band spacing d_{SB} can be derived via:

$$d_{SB} = \cos(\alpha) \times \frac{1}{x}, \quad (2)$$

with l being the height of the deformed region along the compression axis analyzed with an image recognition software (ImageJ), and x being the number of shear bands detected for each sample. Subsequently, the shear-band spacing is averaged for all specimens falling into the same size-bin. **Figure 4**a summarizes the shear-band spacing as a function of sample diameter, exhibiting a linear trend of the form $d_{SB} \approx 0.09 \times d$.

In addition to d_{SB}, the shear-band offset, o_{SB}, was evaluated with $o_{SB} = w / (\cos(\alpha) \times x)$, where w is the increase in sample width at the top of the specimen also quantified with the same image recognition software. It is found that o_{SB} scales similarly as d_{SB} (Figure 4a). A decrease in o_{SB} with decreasing sample size can be directly understood when evaluating the shear-band velocity that is known to scale with specimen size.[20] For the size range covered in Figure 4a, we find a shear-band velocity difference of about a factor of three when derived directly from the displacement-time data. This is in good agreement with the o_{SB}-scaling, and suggests that it is mainly due to a lower shear-band propagation velocity in smaller column sizes, supporting the findings in Ref.[20].

Before turning our attention to the scaling of d_{SB}, and the therein contained consequences for the apparent intermittent-to-homogeneous transition, we note that the size-dependent shear-band spacing very well matches the scaling behavior with a proportionality factor of 0.1 reported by Conner et al. derived from the bending behavior of much larger MG specimens (inset Figure 4a).[31] In the same work a direct correlation between the scaling behavior of shear-band spacing and offset was also observed. By assuming that a shear band behaves like a mode II crack, they found a relation of $d_{SB} \sim o_{SB}/\varepsilon$ with $o_{SB} \sim d$ and therefore also $d_{SB} \sim d$. Whilst the general scaling is in agreement with our data, this correlation is based on considerations for MG samples in a bending geometry, being considerably different to the here conducted nominally uniaxial compression experiments. We also note that MGs have no internal microstructural length scales beyond some short range atomic order, which implies that deformation experiments as a function

Adv. Mater. 2014,
DOI: 10.1002/adma.201401123

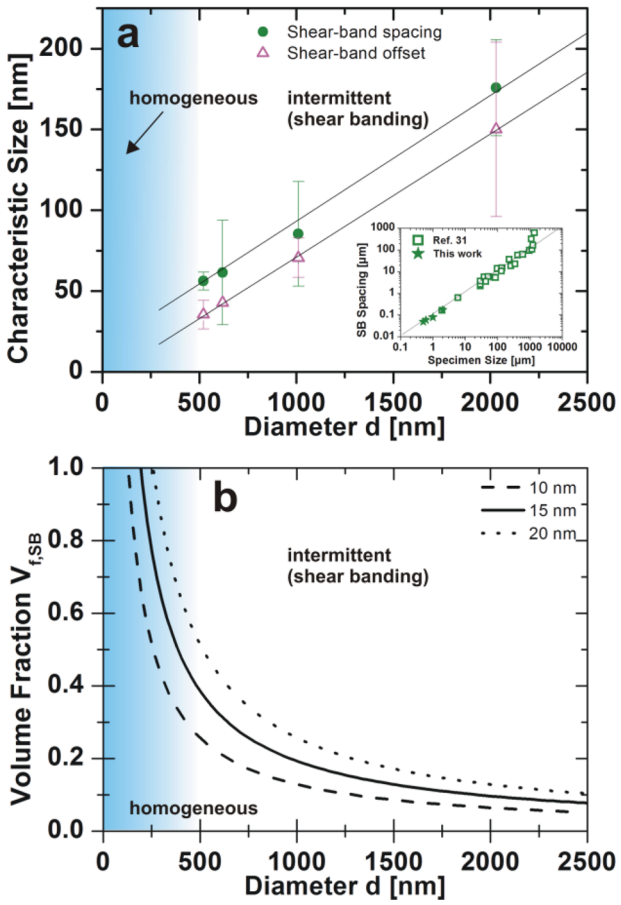

Figure 4. a) Shear-band spacing and offset as a function of sample size. The inset shows that the shear-band offset scales similarly as data by Conner et al.[31] obtained from bending; b) Volume fraction of material inside a shear band as a function of sample size. Depending on the assumed shear-band thickness, $V_{f,SB}$ approaches unity in specimens with diameters in the order of a few hundred nanometers.

of sample size are expected to yield self-similar geometrical scaling as comprised in both d_{SB}- and o_{SB}-trends.

Upon inspection of Figure 4a, it becomes evident that at small sample sizes the shear-band spacing approaches the length scale of the defect itself. Widely accepted values for the shear-band thickness range between 10–20 nm.[36] The shear-band affected volume fraction $V_{f,SB}$ ($V_{f,SB} = t_{SB}/(0.09\times d)$, where t_{SB} is the shear-band thickness) in the deforming columns is now derived from the scaling in Figure 4a, and presented in Figure 4b for three different assumptions of shear-band thicknesses. It is noted that independently of the exact value of the shear-band thickness, the volume fraction of material inside shear bands approaches unity in small specimens. At diameters of ~500 nm the shear-band spacing becomes roughly twice the shear-band thickness itself, which potentially leads to an interaction of neighboring shear bands — a suggestion made by several reports in the framework of self-organized critical behavior of inhomogeneous flow of MG.[37] With decreasing diameter the shear-band affected volumes overlap, imparting deformation into the entire sample volume.

Based on this result, it is a natural consequence to observe a transition between apparent "intermittent" and apparent "homogeneous" deformation behavior, although the underlying deformation mechanism is still governed by the activation and propagation of shear-bands. Since it is well established from shear-band dynamics work[9–11] and modeling[38–40] that the material within a shear-band is in a structurally state comparable to that close to the glass transition, a smooth stress-strain response of a sample with a major volume fraction of shear-band material is indeed expected. Comparing the SRS of $m = 0.05$ with known bulk values yields the indication that the overall mechanical response of the flowing fraction of the glassy material is in a state equivalent to a temperature closer to T_g than to ambient conditions. Indeed, a few tens of degrees below the glass transition, m, derived from bulk testing of MG at ~10^{-3} s^{-1}, drops from values around 0.7–0.9 at T_g to 0.1–0.2,[34,41,42] and reaches values of about ±0.001 at room temperature.[32,35] It is worth to note that m-values of the order of 10^{-3}–10^{-2} are consistently measured when probing very small volumes with nanoindentation at room temperature, where the values strongly depend on the alloy system.[43] Using nanoindentation on our glass and the same analysis as outlined in Ref.[43] we find an m-value of 0.07, as further discussed in the SI.

Although shear-band spacing overlap provides understanding of the intermittent-to-homogeneous transition of small scale metallic glass specimen, two aspects remain to be explored.

Firstly, we observe that the intermittent-to-homogeneous transition is rate dependent; that is, the critical diameter at which apparent homogeneous flow is found, increases with decreasing applied strain rate (Figure 3b). Within the framework of our analysis that the shear-band spacing approaches a value equal to the shear-band thickness, the observed smooth plastic flow of 1 μm size columns compressed at 10^{-4} s^{-1} has to be understood with an increase in the effective shear-band nucleation per unit strain. This is not surprising, given that deformation in MG is thermally activated at all temperatures,[1] which at ambient conditions leads to a higher shear-band density upon decreasing the applied strain rate.[44–46]

Secondly, the propensity of a metallic glass to show "ductile" deformation strongly depends on the internal structural state. With our sputtered PdSi MG film we have explored the un-relaxed end of the accessible range of structural states. Indeed, when annealing the PdSi MG film (590 K, 12 h) under Ar-atmosphere, the 200 nm specimens now fall into the "intermittent" regime and show jerky flow (Figure S2, SI). Hence, reducing the fluctuations in the internal potential energy landscape shifts the apparent intermittent-to-homogeneous transition to smaller diameters. This suggests a sensitivity of the transition in flow behavior to both structural state as well as chemical composition, which may explain the different outcomes of nano- and micro- scale investigations in search of the size-effected flow response. Irreversible plasticity in MG is mediated by local plastic transitions of a group of atoms that have a certain temperature dependent plastic rate. The rate dependent ductile deformation as observed here, conveys hence an interplay between the experimental

time scale (applied rate) and the inherent plastic transition rate of the amorphous structure. Interpreting the local plastic transitions as alpha-transitions, this explanation is well founded in current models describing thermally activated plasticity of MG,[47–49] but does not directly explain the related size-effect. Further investigations are thus required to fully understand the here revealed coupling between size and rate that determine the critical diameter of the intermittent-to-homogeneous transition of small scale metallic glasses.

In summary, we have performed size- and rate-dependent micro-compression tests on PdSi metallic glass columns with diameters between 200 and 2000 nm. A rate-dependent transition in flow response from intermittent to smooth flow behavior was found, and an empirical law describing the transition in a size-rate deformation map is proposed. Choosing a sufficiently low deformation rate allows smooth flow of columns as big as 1 μm in diameter. The strain rate sensitivity m amounts to 0.05 irrespective of sample size and applied rate, suggesting an unaltered underlying deformation mechanism. An analysis of shear-band patterns on inhomogeneously deformed columns indicates that near the transition size in apparent flow behavior the shear-band spacing approaches the internal length scale of the shear-band thickness. We thus attribute the apparent intermittent-to-homogeneous transition to the overlap and interaction of shear bands for columns below the transition size. In combination with a rate-dependent shear-band density, this allows to shift the critical diameter for the intermittent-to-homogeneous transition to higher diameters at very low strain rates.

Experimental Section

Sample preparation: A 5.5 μm thick $Pd_{77}Si_{23}$ MG thin film was fabricated by Argon ion-beam sputtering onto a Si-(100) substrate. The glassy structure was verified by TEM (diffraction mode) and a conventional x-ray θ-2θ scan. Rutherford backscattering spectroscopy was used to determine the chemical composition. Further details on the sample preparation and characterization can be found in Ref. [18]. Micro- and nano-columns were cut with FIB (FEI Nova NanoLab 600) utilizing a 30 kV Ga^+-beam. Consecutive annular milling steps with decreasing beam currents were used to minimize ion-beam damage. A final polishing step with 10 pA or 30 pA was employed for smaller and bigger specimen, respectively. Diameters d ranged between 200 nm and 2000 nm at a fixed aspect ratio of h/d~3 with the column height h. Due to the FIB machining process columns of all sizes show typical deviations from a perfect cylindrical shape. These are a taper of ~3°, rounding at the top end and a slightly sloped shoulder at the bottom end, where the columns are connected to the underlying PdSi metallic glass (all columns with d = 1 μm and smaller). The biggest columns (d = 2 μm) are freestanding on the Si-substrate and are therefore not affected by the bottom shoulder.

Mechanical testing: The columns were tested at room temperature with a nanoindenter (Agilent Nano Indenter G200, DCM I and XP head) equipped with a 10 μm diameter diamond flat punch tip. Loading was performed at constant force rates in open loop load control. Prior to unloading, a 10 s hold segment was used to verify system creeps and drifts. All data sets have been corrected for thermal drift, compliance of the indenter frame, indenter spring stiffness, and elastic substrate compliance. Engineering stress-strain curves were calculated from the force and displacement data using the column diameter d at 50% of the column height h.

Supporting Information

Supporting Information is available from the Wiley Online Library or from the author.

Received: March 12, 2014
Revised: May 19, 2014
Published online:

[1] C. A. Schuh, T. C. Hufnagel, U. Ramamurty, *Acta Mater.* **2007**, *55*, 4067.
[2] A. Inoue, A. Takeuchi, *Mater. Trans.* **2002**, *43*, 1892.
[3] T. D. Shen, R. B. Schwarz, *Appl. Phys. Lett.* **1999**, *75*, 49.
[4] G. Kumar, A. Desai, J. Schroers, *Adv. Mater.* **2011**, *23*, 461.
[5] W. L. Johnson, G. Kaltenboeck, M. D. Demetriou, J. P. Schramm, X. Liu, K. Samwer, C. P. Kim, D. C. Hofmann, *Science* **2011**, *332*, 828.
[6] P. E. Donovan, W. M. Stobbs, *Acta Metall.* **1981**, *29*, 1419.
[7] W. J. Wright, M. W. Samale, T. C. Hufnagel, M. M. LeBlanc, J. N. Florando, *Acta Mater.* **2009**, *57*, 4639.
[8] W. J. Wright, R. R. Byer, X. Gu, *Appl. Phys. Lett.* **2013**, *102*, 241920.
[9] D. Klaumuenzer, A. Lazarev, R. Maass, F. H. Dalla Torre, A. Vinogradov, J. F. Loeffler, *Phys. Rev. Lett.* **2011**, *107*, 185502.
[10] R. Maass, D. Klaumuenzer, J. F. Loeffler, *Acta Mater.* **2011**, *59*, 3205.
[11] R. Maass, D. Klaumuenzer, G. Villard, P. M. Derlet, J. F. Loeffler, *Appl. Phys. Lett.* **2012**, *100*, 071904.
[12] G. Wilde, H. Roesner, *Appl. Phys. Lett.* **2011**, *98*, 251904.
[13] B. P. Kanungo, S. C. Glade, P. Asoka-Kumar, K. M. Flores, *Intermetallics* **2004**, *12*, 1073.
[14] D. C. Hofmann, J.-Y. Suh, A. Wiest, G. Duan, M.-L. Lind, M. D. Demetriou, W. L. Johnson, *Nature* **2008**, *451*, 1085.
[15] J. J. Lewandowski, W. H. Wang, A. L. Greer, *Philos. Mag. Lett.* **2005**, *85*, 77.
[16] W. F. Wu, Y. Li, C. A. Schuh, *Philos. Mag.* **2008**, *88*, 71.
[17] K. Mondal, K. Hono, *Mater. Trans.* **2009**, *50*, 152.
[18] C. A. Volkert, A. Donohue, F. Spaepen, *J. Appl. Phys.* **2008**, *103*, 083539.
[19] D. Jang, C. T. Gross, J. R. Greer, *Int. J. Plast.* **2011**, *27*, 858.
[20] C. Q. Chen, Y. T. Pei, J. T. M. De Hosson, *Acta Mater.* **2009**, *58*, 189.
[21] O. V. Kuzmin, Y. T. Pei, J. T. M. De Hosson, *Scr. Mater.* **2012**, *67*, 344.
[22] J. R. Greer, J. T. M. De Hosson, *Prog. Mater. Sci.* **2011**, *56*, 654.
[23] H. Guo, P. F. Yan, Y. B. Wang, J. Tan, Z. F. Zhang, M. L. Sui, E. Ma, *Nat. Mater.* **2007**, *6*, 735.
[24] B. E. Schuster, Q. Wei, T. C. Hufnagel, K. T. Ramesh, *Acta Mater.* **2008**, *56*, 5091.
[25] A. Dubach, R. Raghavan, J. F. Loeffler, J. Michler, U. Ramamurty, *Scr. Mater.* **2009**, *60*, 567.
[26] D. Klaumuenzer, R. Maass, J. F. Loeffler, *J. Mater. Res.* **2011**, *26*, 1453.
[27] D. J. Magagnosc, R. Ehrbar, G. Kumar, M. R. He, J. Schroers, D. S. Gianola, *Sci. Rep.* **2013**, *3*, 1096.
[28] R. Gerling, F. P. Schimansky, R. Wagner, *Acta Metall.* **1987**, *35*, 1001.
[29] R. Gerling, F. P. Schimansky, R. Wagner, *Scr. Metall.* **1983**, *17*, 203.
[30] Q. Xiao, L. Huang, Y. Shi, *J. Appl. Phys.* **2013**, *113*, 083514.
[31] R. D. Conner, W. L. Johnson, N. E. Paton, W. D. Nix, *J. Appl. Phys.* **2003**, *94*, 904.
[32] M. M. Trexler, N. N. Thadhani, *Prog. Mater. Sci.* **2010**, *55*, 759.
[33] A. Bharathula, S. W. Lee, W. J. Wright, K. M. Flores, *Acta Mater.* **2010**, *58*, 5789.
[34] J. Lu, G. Ravichandran, W. L. Johnson, *Acta Mater.* **2003**, *51*, 3429.
[35] A. Dubach, F. H. Dalla Torre, J. F. Loeffler, *Acta Mater.* **2009**, *57*, 881.

DOI: 10.1002/adma.201401123

[36] A. L. Greer, Y. Q. Cheng, E. Ma, *Mater. Sci. Eng., R* **2013**, *74*, 71.
[37] B. A. Sun, H. B. Yu, W. Jiao, H. Y. Bai, D. Q. Zhao, W. H. Wang, *Phys. Rev. Lett.* **2010**, *105*, 035501.
[38] P. F. Guan, M. W. Chen, T. Egami, *Phys. Rev. Lett.* **2010**, *104*, 205701.
[39] F. Shimizu, S. Ogata, J. Li, *Acta Mater.* **2006**, *54*, 4293.
[40] A. J. Cao, Y. Q. Cheng, E. Ma, *Acta Mater.* **2009**, *57*, 5146.
[41] Y. Kawamura, T. Shibata, A. Inoue, T. Masumoto, *Scr. Mater.* **1997**, *37*, 431.
[42] Y. Kawamura, T. Nakamura, A. Inoue, *Scr. Mater.* **1998**, *39*, 301.
[43] D. Pan, A. Inoue, T. Sakurai, M. W. Chen, *Proc. Natl. Acad. Sci. USA* **2008**, *105*, 14769.
[44] W. H. Jiang, G. J. Fan, F. X. Liu, G. Y. Wang, H. Choo, P. K. Liaw, *Int. J. Plast.* **2008**, *24*, 1.
[45] W. H. Jiang, G. J. Fan, F. X. Liu, G. Y. Wang, H. Choo, P. K. Liaw, *J. Mater. Res.* **2006**, *21*, 2164.
[46] H. Zhang, S. Maiti, G. Subhash, *J. Mech. Phys. Solids* **2008**, *56*, 2171.
[47] P. M. Derlet, R. Maass, *Philos. Mag.* **2013**, *93*, 4232.
[48] D. Rodney, C. A. Schuh, *Phys. Rev. B* **2009**, *80*, 184203.
[49] W. L. Johnson, K. Samwer, *Phys. Rev. Lett.* **2005**, *95*, 195501.